2018

R1233zd(E) and R245fa Flow Boiling Heat Transfer and Pressure Drop inside a 4.2 mm ID Microfin Tube

Giovanni A. Longo
tony@gest.unipd.it

Andrea Diani
simone.mancin@unipd.it

Giulia Righetti
Dept. of Management and Engineering, University of Padova, Italy, righetti@gest.unipd.it

Claudio Zilio
University of Padova - DTG, Italy, claudio.zilio@unipd.it

R1233zd(E) and R245fa Flow Boiling Heat Transfer and Pressure Drop inside a 4.2 mm ID Microfin Tube

Simone MANCIN*, Giulia RIGHETTI, Claudio ZILIO, Giovanni A. LONGO
Dept. of Management and Engineering, University of Padova
Str.lla S. Nicola, 3, VICENZA, 36100-Italy

simone.mancin@unipd.it, giulia.righetti@unipd.it, claudio.zilio@unipd.it, tony@gest.unipd.it

* Corresponding Author

ABSTRACT

This paper presents R1233zd(E) and R245fa flow boiling heat transfer and pressure drop measurements inside a mini microfin tube with an internal diameter at the fin tip equal to 4.2 mm, having 40 fins, 0.15 mm high, and a helix angle of 18°. The tube was brazed inside a copper plate and electrically heated from the bottom. The experimental measurements were carried out at a constant mean saturation temperature of 30 °C, by varying the refrigerant mass velocity between 100 and 300 kg m^{-2} s^{-1}, the mean vapor quality from 0.1 and 0.95, and the heat flux from 15 to 90 kW m^{-2}. The experimental results are here presented in terms of two-phase heat transfer coefficient and frictional pressure drop. In this paper, the performance of the two fluids is compared under different working conditions and commented. Finally, the experimental measurements were used to assess some models for boiling heat transfer coefficient and frictional pressure drop estimations available in the open literature.

1. INTRODUCTION

The subject of this paper is the new HydroChloroFluoroOlefin (HCFO) molecule R1233zd(E) proposed to be an environmentally friendly substitute to R245fa, thanks to its very low GWP (GWP<7, www.epa.gov), its near zero ODP (ODP= 0.00024-0.00034, www.epa.gov), and its very short atmospheric lifetime (about 26 days, Romeo *et al.*, 2017). It is also non-flammable, and it exhibits favorable thermophysical properties (see Table 1, where the main R1233zd(E) and R245fa physical properties involved in the heat transfer evaluated according to Lemmon *et al.* (2017) are reported and compared).

Table 1. Main R1233zd(E) and R245fa thermophysical properties involved in heat transfer and fluid flow at t_{sat}= 30°C, evaluated according to Lemmon *et al.* (2017).

Properties		**R1233zd(E)**	**R245fa**
Critic pressure, p_{crit} [bar]		36.24	36.51
Saturation pressure, p_{sat} [bar]		1.55	1.78
Density, ρ [kg m^{-3}]	Liquid	1250.6	1324.8
	Vapor	8.5	10.1
Thermal Conductivity, λ [W m^{-1} K^{-1}]	Liquid	0.081	0.087
	Vapor	0.011	0.013
Dynamic viscosity, μ [μPa s]	Liquid	272.1	374.8
	Vapor	10.2	10.5
Surface tension [mN m^{-1}]		13.91	12.98
Latent heat of vaporization [kJ kg^{-1}]		188.52	188.33
Reduced pressure, p_{red} [-]		0.0427	0.0488

Despite some authors have already suggested R1233zd(E) as viable option to substitute R245fa (see for instance, Guillaume *et al.*, 2017), no comparison between R1233zd(E) and R245fa is available during two phase flow inside a tube, even if these tubes are the main components of a large number of heat exchangers. Huang and Thome (2017) examined R1233zd(E), R245fa, and R236fa two phase pressure drop in a multi microchannel evaporator (10 mm long and 10 mm wide, having 67 parallel channels, 100 x 100 μm^2 each) at mass fluxes from 1250 to 2750 kg m^{-2} s^{-1} and heat fluxes from 200 to 640 kW m^{-2}. R236fa exhibited the lowest channel pressure drop due to its smallest liquid to vapor density ratio and liquid viscosity, while R1233zd(E) and R245fa were comparable. No heat transfer data were presented.

Furthermore, just few R1233zd(E) data were published during flow boiling inside a microfin tube. At the best Authors' knowledge, just Longo *et al.* (2017a) presented some R1233zd(E) flow boiling inside a ID 4.3 mm microfin tube data, collected at 30 °C of saturation temperature, mass velocities from 100 kg m^{-2} s^{-1} and 300 kg m^{-2} s^{-1}, and heat fluxes from 15 to 90 kW m^{-2}. More in general, since their invention by Fujie *et al.* (1977), microfin tubes were largely studied, but the available literature about small diameter microfin tubes (i.e. inner diameter lower than 6 mm or so) is still limited if compared to larger tubes, as reported also in the thorough review by Righetti *et al.* (2016).

In this paper new experimental data of R1233zd(E) flow boiling inside a mini microfin tube (ID 4.2 mm) are presented and compared against others of R245fa, obtained under the same working conditions. All the data points were collected at a constant mean saturation temperature 30 °C, by varying the refrigerant mass velocity between 100 kg m^{-2} s^{-1} and 300 kg m^{-2} s^{-1}, the vapor quality from 0.2 to 0.95, and the heat flux from 15 to 90 kW m^{-2}. The experimental results are presented in terms of two-phase heat transfer coefficient, onset dryout vapor quality, and frictional pressure drop. Finally, some literature correlations were implemented and the results compared against the collected experimental values.

2. EXPERIMENTAL SET UP AND TEST SECTION

The experimental test facility, located in the Nano Heat Transfer Lab at the Management and Engineering Department of the University of Padova, was designed for heat transfer and pressure drop measurements and flow visualization during flow boiling of pure refrigerants and refrigerants mixtures inside structured micro- and nano-geometries. As shown in Figure 1, it consists of three loops: the main one, where the pumped refrigerant flows, and two auxiliary cooling water and hot water loops which serve the heat exchangers placed in the main loop. The refrigerant is pumped through the circuit by means of a variable speed volumetric gear pump, then it is vaporized in a Brazed Plate Heat Exchanger (BPHE) fed with hot water to achieve the desired value of vapor quality. The hot water is supplied by a thermostatic bath; both water flow rate and water temperature can be independently set. The heat flow rate exchanged at the BPHE evaporator is accurately measured by means of a magnetic flow meter and a calibrated T-type thermopile; furthermore, preliminary tests were run to verify the heat balance between refrigerant and water sides, the results showed a misbalance always less than 2%.
The refrigerant enters the microfin test tube at a known mass velocity and vapor quality and then it is vaporized by means of a calibrated Ni-Cr wire resistance. The electrical power supplied to the sample is indirectly measured by means of a calibrated reference resistance (shunt) and by the measurement of the electrical difference potential of the resistance wire inserted in the copper heater. The current can be calculated from the Ohm's law. The fluid leaves the test section and enters in a post-condenser, a brazed plate heat exchanger fed with tap water, where it is fully condensed and subcooled. A damper connected to the compressed air line operates as pressure regulator to control the saturation conditions in the refrigerant loop.

As shown in Figure 1, the refrigerant pressure and temperature are measured at several locations throughout the circuit to know the refrigerant properties at the inlet and outlet of each heat exchanger. The refrigerant mass flow rate can be independently controlled by the gear pump and it is measured by means of a Coriolis effect flowmeter. No oil circulates in the refrigerant loop.
Table 2 lists the values of uncertainty (k=2) of the instruments used in the experimental facility. The mini microfin tube was brazed inside a guide milled on the top surface of a copper plate, which is 200 mm long, 10 mm wide, and 20 mm high. 16 holes were drilled just 1 mm below the microfin tube, in order to locate as many T-type thermocouples to monitor the wall temperature distribution.

Table 2. Instruments uncertainty.

Transducer	Uncertainty (k=2)
T-type thermocouples	± 0.1 K
T-type thermopiles	± 0.05 K
Electric power	± 0.26% of the reading
Coriolis mass flowmeter (refrigerant loop)	± 0.10% of the reading
Magnetic volumetric flowmeter (hot water loop)	± 0.2% of FS= 0.33 10^{-3} m^3 s^{-1}
Differential pressure transducer (test section)	± 0.075% of FS= 0.3 MPa
Absolute pressure transducers	± 0.065% of FS= 4 MPa

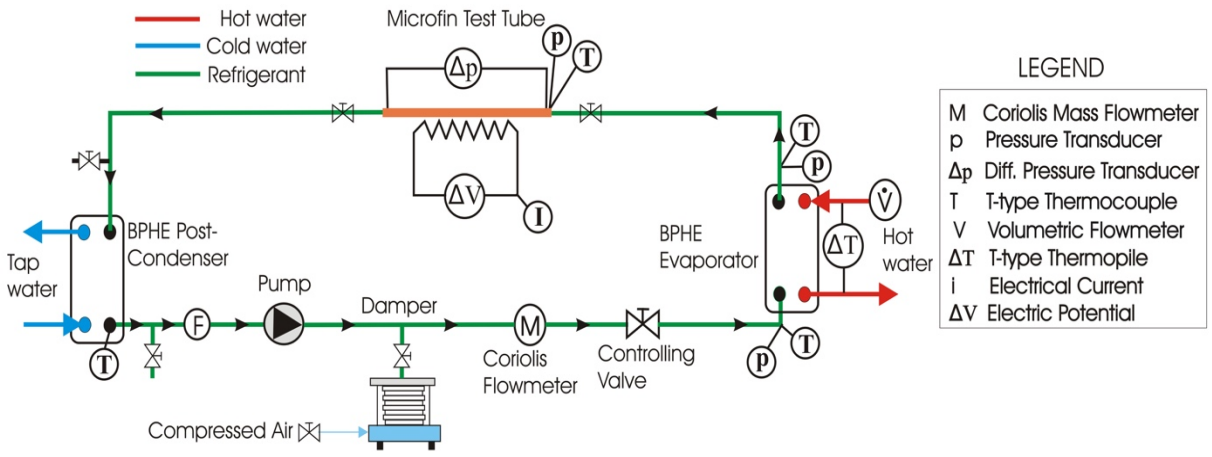

Figure 1: Schematic of the experimental setup.

Table 3: Microfin tube geometry.

Characteristic	Value
Outer Diameter	5 mm
Fin Tip Diameter, D	4.2 mm
Apex angle, γ	42°
Helix angle, β	18°
Number of fin, n	40
Fin height, h	0.15 mm
Tube thickness	0.23 mm

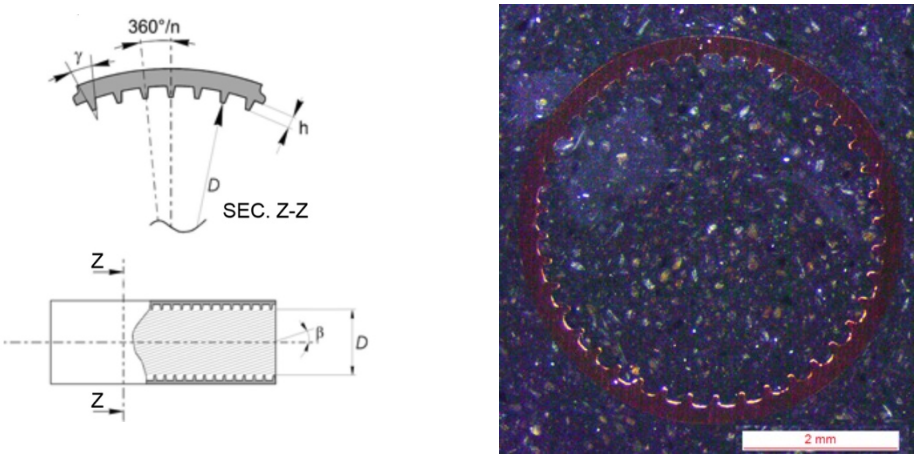

Figure 2: Schematic and photo of the microfin tube.

Another guide was milled on the bottom side of the copper plate, to host a Nickel-Chrome wire resistance connected to a DC current generator, which supplies the electrical power needed to vaporize the refrigerant flowing inside the tube. In order to avoid the abrupt pressure drops due to flow contraction and expansion, a suitable smooth connection to the refrigerant circuit having the same fin tip diameter (D=4.2 mm) was designed and realized to join the test tube with inlet and outlet pipes. Pressure ports are located about 25 mm downstream and upstream of the copper plate, thus the length for pressure drop measurements is 250 mm. The test section is located inside an aluminum housing filled with 15 mm thick ceramic fiber blanket, to limit as much as possible the heat losses due to conduction to the ambient. Figure 2 and Table 2 summarize the main geometrical characteristics of the tested tube. Given the reported dimensions, the area enhancement with reference to the smooth tube having the same fin tip diameter is equal to 1.62.
For further details on the experimental set up and test section the reader could refer to Longo *et al.* (2017a) and Longo *et al.* (2017b).

3. DATA REDUCTION

As described in the previous section, the subcooled liquid pumped by the magnetically coupled gear pump is vaporized into a BPHE fed with hot water. Thus, the vapor quality at the inlet of the test section can be calculated from a thermal balance at the evaporator, as:

$$q_{evap} = \dot{m}_w \cdot c_{p,w} \cdot \left(t_{w,in} - t_{w,out}\right) = \dot{m}_r \cdot \left(J_{in,TS} - J_{L,sub}\right) \quad \text{Eq. (1)}$$

where $\dot{m}_w$ is the water mass flow rate, $c_{p,w}$ is the specific heat capacity of the water, $t_{w,in}$ and $t_{w,out}$ are the inlet and outlet water temperatures. The right-hand side term of Eq. (1) reports the refrigerant side heat flow rate where $\dot{m}_r$ is the refrigerant mass flow rate while $J_{in,TS}$ and $J_{L,sub}$ are the unknown specific enthalpy at the inlet of the test section and the specific enthalpy of the subcooled liquid entering the BPHE, respectively. Once calculated $J_{in,TS}$, the vapor quality at the inlet of the test section can be estimated by:

$$x_{in,TS} = \frac{J_{in,TS} - J_L}{J_V - J_L} \quad \text{Eq. (2)}$$

where J_L and J_V are the specific enthalpies of the saturated liquid and vapor, respectively, evaluated at the saturation pressure of the refrigerant measured at the inlet of the test section. As already described, the electrical power supplied to the sample is indirectly measured by means of a calibrated reference resistance (shunt) and by the measurement of the effective electrical difference potential of the resistance wire inserted in the copper heater. Preliminary heat transfer measurements permitted to estimate the heat loss (q_{loss}) due to conduction through the test section as a function of the mean wall temperature. The tests were run under vacuum conditions on the refrigerant channel by supplying the power needed to maintain the mean wall temperature at a set value. The measurements were carried out by varying the mean wall temperature from 28 °C to 63 °C. The results showed that the heat loss increases linearly as the mean wall temperature increases (R>0.99). In the tested range of wall temperature, the heat loss by conduction through the test section can be estimated by:

$$|q_{loss}| = 0.2006 \cdot \bar{t}_{wall}\ [°C] - 4.6698 \quad [W] \quad \text{Eq. (3)}$$

thus, the actual heat flow rate q_{TS} supplied to the sample is given by:

$$q_{TS} = P_{EL} - |q_{loss}| = \Delta V \cdot I - |q_{loss}| \quad \text{Eq. (4)}$$

It is worth underlying that the q_{loss} varied from 1.0% to 4.6% of the electrical power supplied. The mean vapor quality, x_{mean} is the average value between the inlet and outlet ones. The two-phase heat transfer coefficient HTC, referred to the nominal area A, can be defined as:

$$HTC = \frac{q_{TS}}{A \cdot (\bar{t}_{wall} - \bar{t}_{sat})} = \frac{q_{TS}}{\pi \cdot D \cdot L \cdot (\bar{t}_{wall} - \bar{t}_{sat})} \quad \text{Eq. (5)}$$

where $\bar{t}_{wall}$ and $\bar{t}_{sat}$ are defined by the followings:

$$\bar{t}_{wall} = \frac{1}{16}\sum_{i=1}^{16} t_{wall,i} \text{ and } \bar{t}_{sat} = \frac{t_{sat,in}(p_{sat,in})+t_{sat,out}(p_{sat,out})}{2} \quad \text{Eq. (6)}$$

The hydraulic performance of the microfin tube is given in terms of frictional pressure drop, which was calculated from the measured total pressure drop by subtracting the momentum pressure and gravity pressure drops, as:

$$\Delta p_f = \Delta p_t - \Delta p_c - \Delta p_a \quad \text{Eq. (7)}$$

The momentum pressure drops are estimated by the homogeneous model for two-phase flow as follows:

$$\Delta p_a = G^2(v_V - v_L)\,|\Delta x| \quad \text{Eq. (8)}$$

where G is the refrigerant mass flux, v_L and v_V are the specific volume of liquid and vapor phase, $|\Delta x|$ is the absolute value of the vapor quality change through the whole test section. The gravitational contribution Δp_c is equal to 0 Pa because the microfin tube is horizontally located. Thermodynamic and transport properties are estimated from RefProp v9.4 (Lemmon et al., 2017). A detailed error analysis was performed in accordance with Kline and McClintock (1953) using the values of the uncertainty of the instruments listed in Table 1; it was estimated that the uncertainty (k=2) on the two-phase heat transfer coefficient showed a mean value of around ±8%, while the uncertainty on the vapor quality was ±0.03. The pressure drops showed a mean uncertainty of around 8%.

4. EXPERIMENTAL RESULTS

Table 1 lists the main thermo-physical properties involved in the heat transfer of R1233zd(E) and R245fa at 30 °C of saturation temperature evaluated according RefProp 10, Lemmon *et al.* (2017). Both fluids have a critical pressure around 36 bar, so at the operating conditions under investigation (t_{sat}=30°C), they have a very low reduced pressure, around 0.04. Furthermore, they present a notable difference between the liquid and vapor densities (ρ_L/ρ_V=147 and 131 for R1233zd(E) and R245fa, respectively), and a great surface tension (around 13 mN m^{-1}).

Flow boiling heat transfer coefficient is mainly related to reduced pressure (0.043 vs. 0.049 for R1233zd(E) and R245fa, respectively), liquid thermal conductivity (0.081 vs. 0.087 W m^{-1} K^{-1} for R1233zd(E) and R245fa, respectively) and vapor/liquid densities. So, it is fair to expect a R1233zd(E) similar or slightly lower performance than R245fa. On the other hand, pressure drop is connected to the liquid and vapor density ratio, liquid density and viscosity, and the reduced pressure. Again, the two refrigerants present similar values, but the R1233zd(E) could exhibit slightly higher pressure drops due to a lower vapor density (i.e., 1250 kg m^{-3} vs. 1324 kg m^{-3} for R1233zd(E) and R245fa, respectively) and a lower saturation pressure (-15%). Finally, at these operating conditions, since both the fluids have a very low vapor density, a high surface tension, and a low reduced pressure, the forced convective boiling contribution should be more relevant as compared to nucleate boiling one during the vaporization process. These considerations are here confirmed by the experimental results presented in what follows.

The following figures represent a comparison between R1233zd(E) and R245fa heat transfer coefficient at a saturation temperature of 30 °C, under the same working conditions.

Figure 3 plots the data at heat flux (HF) equal to 15 W m^{-2} and mass velocity (G) of 100 kg m^{-2} s^{-1}. Accordingly, Figure 4 shows data at the same heat flux (HF=15 W m^{-2}) but a higher mass velocity equal to 200 kg m^{-2} s^{-1}. Both the graphs present similar heat transfer behavior, in fact the heat transfer coefficients increase with the vapor quality, meaning that forced convection is affecting the phase-change process at this low heat flux. This contribution is stronger at higher mass velocity, as a result the slope at G=200 kg m^{-2} s^{-1} increases. No considerable differences can be appreciated between the refrigerants in terms of absolute values and trend. By further increasing the mass velocity (Figure 5, G=300 kg m^{-2} s^{-1}, HF=15 W m^{-2}, t_{sat}=30°C), the slope of both refrigerants appears lower, probably due to the effect caused by an increment in pressure drop that deteriorates the heat transfer performance (see Figure 7 where frictional pressure drops for many mass velocities are presented). In addition, due to a higher mass velocity, the thermal crisis was not observed; this result can be attributed to the presence of the microfins, which extend and promote stable and continuous boiling mitigating the dryout phenomenon. The two fluids have similar performance despite the differences in thermophysical properties.

Figure 6 presents data collected at G=300 kg m^{-2} and a fixed heat flux equal to 90 W m^{-2}. The heat transfer coefficients obtained are almost constant, perhaps affected by the pressure drop that becomes even higher. Again, the refrigerants have similar trend and dry out inception.

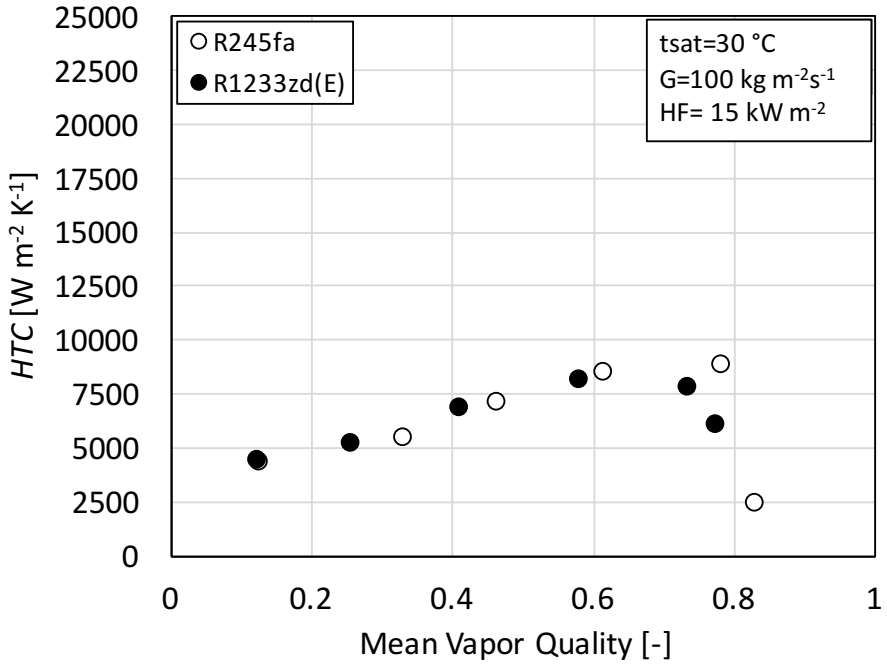

Figure 3. Comparison between R1233zd(E) and R245fa heat transfer coefficients at mass velocity=100 kg m^{-2} s^{-1}, heat flux=15 kW m^{-2}, and saturation temperature= 30°C.

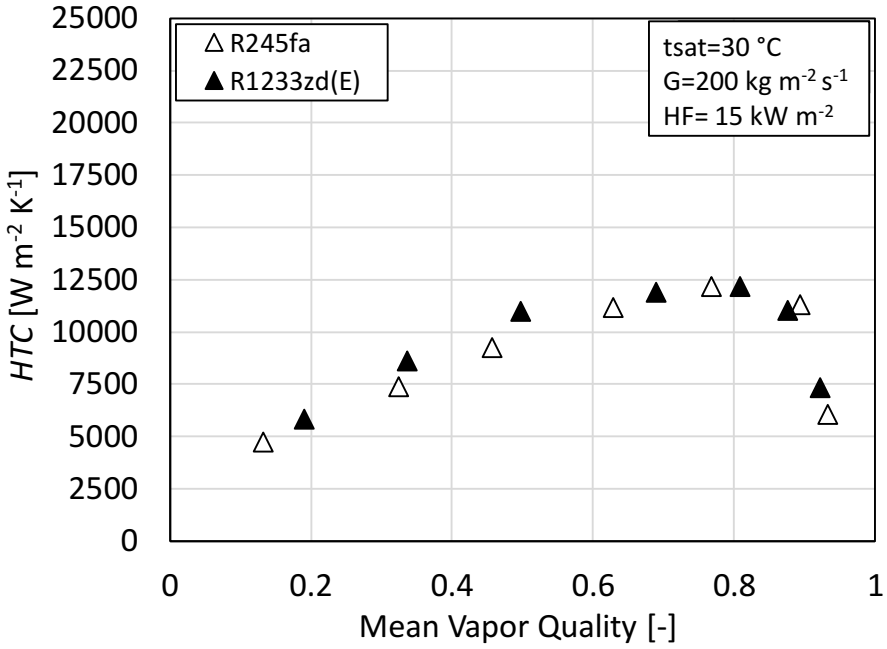

Figure 4. Comparison between R1233zd(E) and R245fa heat transfer coefficients at mass velocity=200 kg m^{-2} s^{-1}, heat flux=15 kW m^{-2}, and saturation temperature= 30°C.

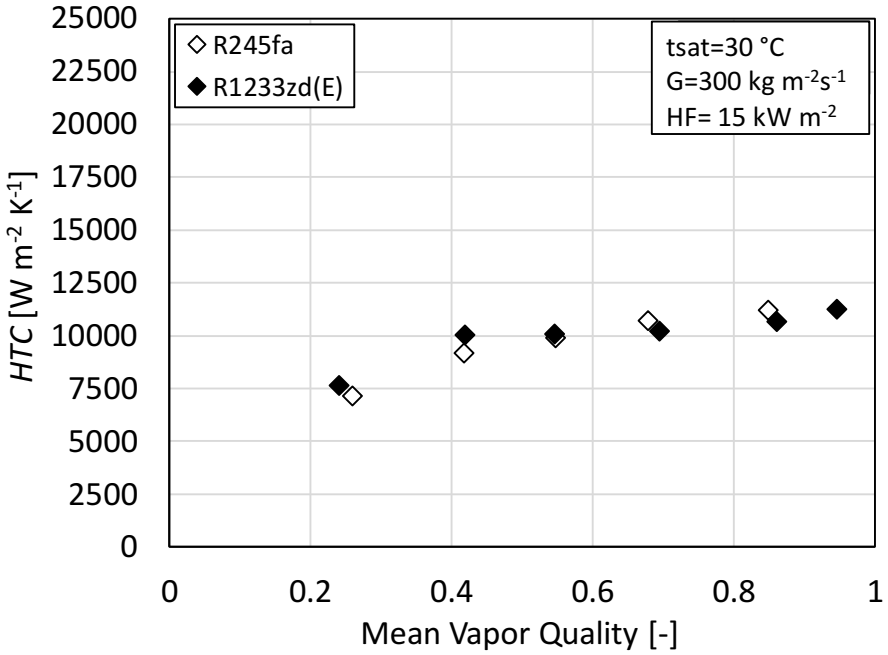

Figure 5. Comparison between R1233zd(E) and R245fa heat transfer coefficients at mass velocity=300 kg m^{-2} s^{-1}, heat flux=15 kW m^{-2}, and saturation temperature= 30°C.

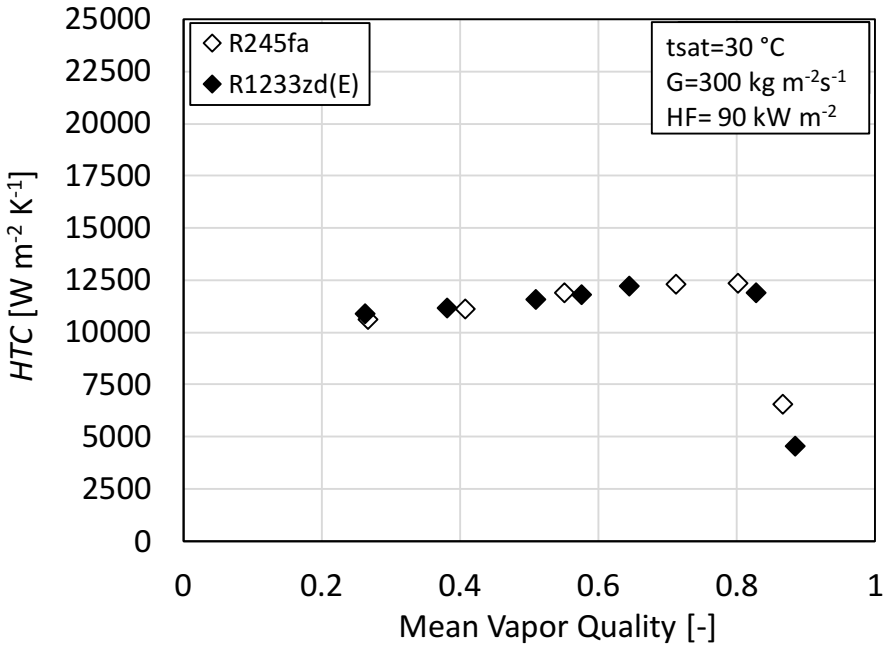

Figure 6. Comparison between R1233zd(E) and R245fa heat transfer coefficients at mass velocity=300 kg m^{-2} s^{-1}, heat flux=90 kW m^{-2}, and saturation temperature= 30°C.

On the other hand, Figure 7 shows the comparison between R1233zd(E) and R245fa frictional pressure gradients at *HF*=15 W m^{-2} and t_{sat}=30 °C and several mass velocities (*G* ranging from 100 to 300 kg m^{-2} s^{-1}). Under this point of view, R1233zd(E) displays higher pressure drops, on average +16%. This could be explained considering the difference in saturation pressure and vapor density as previously presented (Table 1). As expected, at constant mass velocity, the frictional pressure gradient increases with vapor quality. Furthermore, at constant vapor quality, it increases as the mass velocity increases.

All the data collected were finally compared against some models available in the literature for two-phase heat transfer coefficient and pressure drop in microfin tubes. The models by Padovan *et al.* (2011), Diani *et al.* (2014), and Rollmann and Splider (2016) were chosen for the flow boiling heat transfer coefficient assessment, while the ones by Haraguchi *et al.* (1993), Kedzierski and Goncalves (1999), Cavallini *et al.* (2000), Miyara *et al.* (2000), Goto *et al.* (2001), Bandarra Filho *et al.* (2004), Oliver *et al.* (2004), and Diani *et al.* (2014) were selected to be compared against the experimental two-phase frictional pressure gradients. In terms of heat transfer coefficient, the Rollmann and Splider (2016) model presents the best agreement with both the fluids. The relative deviation is around 0.1% and -5.6% for R1233zd(E) and R245fa, respectively. Besides, in terms of frictional pressure gradient, the Haraguchi *et al.* (1993) correlation obtains the lower relative deviations (i.e., -4.1% and -8.6% for R1233zd(E) and R245fa, respectively), while the Cavallini *et al.* (2000) model presents the lower absolute deviations (i.e., 26% and 19.1% for R1233zd(E) and R245fa, respectively).

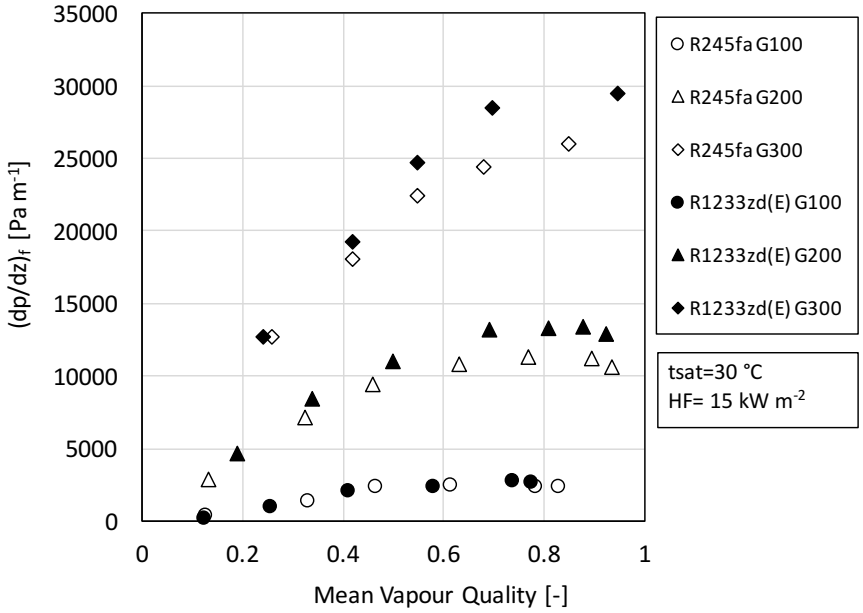

Figure 7. Comparison between R1233zd(E) and R245fa frictional pressure gradients at different mass velocities, heat flux=15 kW m^{-2}, saturation temperature= 30°C.

5. CONCLUSIONS

The paper presents experimental heat transfer coefficients and pressure drops measured during R1233zd(E) and R245fa flow boiling inside a mini microfin tube with an inner diameter at the fin tip of 4.2 mm. Tests were run at a constant mean saturation temperature of 30 °C, by varying the vapor quality from 0.2 to 0.95, the mass velocity from 100 to 300 kg m^{-2} s^{-1}, and the heat flux from 15 to 90 kW m^{-2}.

The performance of both fluids was compared under similar working conditions. Concerning heat transfer coefficient, no considerable differences can be appreciated between the two refrigerants in terms of absolute value and trend.

Considering the frictional pressure drops, R1233zd(E) displays average +16% higher values as compared to R245fa; this could be explained with the difference in saturation pressure and vapor density.

All the data collected were finally compared against some models available in the literature for two-phase heat transfer coefficient and frictional pressure gradient in microfin tubes. In terms of heat transfer coefficient, the Rollmann and Splider (2016) model presents the best agreement with both the fluids. The relative deviation is around 0.1% and

-5.6% for R1233zd(E) and R245fa, respectively. Besides, in terms of frictional pressure gradient, the Haraguchi *et al.* (1993) correlation exhibits the lower relative deviations (i.e., -4.1% and -8.6% for R1233zd(E) and R245fa, respectively), while the Cavallini *et al.* (2000) model presents the lower absolute deviations (i.e., 26% and 19.1% for R1233zd(E) and R245fa, respectively).

NOMENCLATURE

A	area	(m^2)	b	helix angle	(°)
c_p	specific heat capacity	($J\ kg^{-1}\ K^{-1}$)	γ	apex angle	(°)
D	fin tip diameter	(m)	λ	thermal conductivity	($W\ m^{-1}\ K^{-1}$)
G	mass velocity	($kg\ m^{-2}\ s^{-1}$)	μ	dynamic viscosity	(Pa s)
h	fin height	(m)	σ	surface tension	($N\ m^{-1}$)
HTC	heat transfer coefficient	($W\ m^{-2}\ K^{-1}$)	**Subscript**		
HF	heat flux	($W\ m^{-2}$)	in	inlet	
J	specific enthalpy	($J\ kg^{-1}$)	f	frictional	
k	coverage factor	(-)	L	liquid	
L	heated length	(m)	out	outlet	
$\dot{m}$	mass flow rate	($kg\ s^{-1}$)	r	refrigerant	
n	fin number	(-)	TS	Test section	
n	fin number	(-)	w	water	
p	pressure	(Pa)	evap	vaporization	
P	power	(W)	sub	subcooled	
q	heat flow rate	(W)	V	vapor	
r	latent heat of vaporization	($J\ kg^{-1}$)	loss	losses	
s	thickness	(m)	EL	electrical	
t	temperature	(°C)	wall	wall	
v	specific volume	($m^3\ kg^{-1}$)	sat	saturation	
x	vapor quality	(-)	t	total	
Greek symbol			a	momentum	
Δ	variation	(-)	c	gravitational	

REFERENCES

Bandarra Filho, E.P., Saiz Jabardo, J.M., Barbieri, P.E.L., (2004). Convective boiling pressure drop of refrigerant R-134a in horizontal smooth and microfin tubes, *International Journal of Refrigeration,* 27, 895–903.

Cavallini, A., Del Col, D., Doretti, L., Longo, G.A., Rossetto, L., (2000). Heat transfer and pressure drop during condensation of refrigerants inside horizontal enhanced tubes, *International Journal of Refrigeration,* 23, 4-25.

Diani, A., Mancin, S., Rossetto, L., (2014), R1234ze(E) flow boiling inside a 3.4 mm ID microfin tube, *Int J. Refrigeration,* 47, 105-119.

Fujie, K., Itoh, N., Kimura, H., Nakayama, N., Yanugi, T., (1977). Heat transfer pipe, US Patent 4044797, assigned to Hitachi.

Goto, M., Inoue, N., Ishiwatari, N., (2001). Condensation and evaporation heat transfer of R410A inside internally grooved tubes, *International Journal of Refrigeration,* 24, 628-638.

Guillaume, L., Legros, A., Desideri, A., Lemort, V., (2017). Performance of a radial-inflow turbine integrated in an ORC system and designed for a WHR on truck application: An experimental comparison between R245fa and R1233zd, *Applied Energy,* 186, 408–422.

Haraguchi, H., Koyama, S., Esaki, J., Fujii, T., (1993). Condensation heat transfer of refrigerants HFC134a, HCFC123 and HCFC22 in a horizontal smooth tube and a horizontal microfin tube, 30th *National Symp of Japan, Yokohama,* 343-345.

Huang, H., Thome J.R., (2017). An experimental study on flow boiling pressure drop in multi microchannel evaporators with different refrigerants, *Experimental Thermal and Fluid Science,* 80, 391–407.

Kedezierski, M.A., Goncalves, 1999, J.M., Horizontal convective condensation of alternative refrigerants within a micro-fin tube, *Journal of Enhanced Heat Transfer,* 6, 161-178.

Kline, S.J., McClintock, F.A., (1953). Describing uncertainties in single-sample experiments, *Mech. Eng.,* vol. 75: p.

3–8.
Lemmon, E.W., Bell, I.H., Huber, M.L., McLinden, M.O., (2017). NIST Standard Reference Database 23 Beta Version (Aug. 23, 2017): Reference Fluid Thermodynamic and Transport Properties- REFPROP, Version 9.4.4.03, National Institute of Standards and Technology, Standard Reference Data Program, Gaithersburg.
Longo, G.A., Mancin, S., Righetti, G., Zilio, C., (2017a). R1233zd(E) flow boiling inside a 4.3 mm ID microfin tube. In: *5th IIR International Conference on Thermophysical Properties and Transfer Processes of Refrigerants,* 23-26 Aprile, 2017, Seoul, Korea. DOI: 10.18462/iir.tptpr.2017.0023.
Longo G. A., Mancin S., Righetti G., Zilio C., Doretti L., (2017b). Saturated R134a flow boiling inside a 4.3 mm inner diameter microfin tube, *Science and Technology for the Built Environment,* ISSN: 2374-474X. DOI: 10.1080/23744731.2017.1300012
Miyara, A., Nonaka, K., Taniguchi, M., (2000). Condensation heat transfer and flow pattern inside a herringbone-type micro-fin tube, International Journal of Refrigeration, 23, 141-152.
Oliver, J.A., Liebenberg, L., Kedzierski, M.A., Meyer, J.P., (2004). Pressure drop during refrigerant condensation inside horizontal smooth, helical microfin, and herringbone microfin tubes*, Journal of Heat Transfer,* 126, 687-696.
Padovan, A., Del Col, D., Rossetto, L., (2011). Experimental study on flow boiling of R134a and R410A in a horizontal microfin tube at high saturation temperatures, *Applied Thermal Engineering,* 31, 3814–3826.
Righetti, G., Zilio, C., Mancin, S., Longo, G.A., (2016). A review on in-tube two-phase heat transfer of hydro-fluoro-olefines refrigerants, *Science and Technology for the Built Environment,* 22 (8), 1191-1225
Rollmann P., Spindler, K., (2016). New models for heat transfer and pressure drop during flow boiling of R407C and R410A in a horizontal microfin tube, *International Journal of Thermal Sciences,* 103, 57-66.
Romeo, R., Giuliano Albo, P.A., Lago, S., Brown, J.S., (2017). Experimental liquid densities of cis-1,3,3,3-tetrafluoroprop-1-ene (R1234ze(Z)) and trans-1-chloro-3,3,3-trifluoropropene (R1233zd(E)), *International Journal of Refrigeration,* 79 176–182.
www.epa.gov, United States Environmental Protection Agency web site.

ACKNOWLEDGEMENT

This research project was partially funded by: CariVerona Foundation, Verona, Italy, Ricerca Scientifica e Tecnologica 2016-2019: "Sostenibilità e autenticazione nutrizionale di filiere lattiero-casearie a tutela del consumatore". The authors are very grateful to Dr. Eric Lemmon of NIST (Boulder, Colorado) for making available in advance of the official release of RefProp 10.0 and for his advice. The supports of CENTRAL GLASS CO. ltd for donating the fluid and of Wieland-Werke AG (Christoph Walther) for donating the tube samples are gratefully acknowledged. Generalmeccanica Snc and Dr. Damiano Soprana are gratefully acknowledged for their valuable help in the manufacturing of the test section.